ISSN 1009 – 3095 *Journal of Zhejiang University SCIENCE* V.3, No.2, P.157 – 161, Apr. – June, 2002
http://www.periodicals.com.cn; http://www.zju.edu.cn/English
http://www.zjupress.com; http://lib.zju.edu.cn/eindex.htm; jzu_s@mail.hz.zj.cn

Simulating confined swirling gas-solid two phase jet*

JIN Han-hui(金晗辉), XIA Jun(夏　钧), FAN Jian-ren(樊建人)†, CEN Ke-fa(岑可法)

(*Department of Energy Engineering, Zhejiang University, Hangzhou, 310027, China*)

Received May 21, 2001; revision accepted July 28, 2001

Abstract: A k-ε-k_p multi-fluid model was used to simulate confined swirling gas-solid two phase jet comprised of particle-laden flow from a center tube and a swirling air stream entering the test section from the coaxial annular. After considering the drag force between the two phases and gravity, a series of numerical simulations of the two-phase flow of 30μm, 45μm, 60μm diameter particles were performed on a $x \times r = 50 \times 50$ mesh grid respectively. The results showed that the k-ε-k_p multi-fluid model can be applied to predict moderate swirling multi-phase flow. When the particle diameter is large, the collision of the particles with the wall will influence the prediction accuracy. The bigger the diameter of the particles, the stronger the collision with the wall, and the more obvious the difference between measured and calculated results.

Key words: A k-ε-k_p multi-fluid model, Two phase flow, Confined swirling jet
Document code: A　　**CLC number:** TK16

INTRODUCTION

Confined swirling two phase flows are widely utilized in engineering applications, such as combustion systems, cyclone separators, etc. They are used to enhance the flame stability and to mix properly the fuel and oxidizer in combustion systems. In cyclone separators they are used to separate particles by centrifugal force. In all of those engineering systems, the behavior of both the particles and the air is of great importance.

Studies were carried out to find the flow characteristics of the particles and the air through experiment and numerical simulation (Sommerfeld et al., 1993; Zha, 2000; He, 2000). In their numerical studies, the flow characteristics of the particles were investigated by using the Lagrangian approach, which showed that interaction between the particle phase and the air phase mainly depended on the local eddy lifetime and the stokesian response time of the particles. More than 100 000 particles were needed to describe the flow characteristics of the particle phase (Crowe, 1985). This paper presents numerical simulation by using the k-ε-k_p multi-fluid model with the particle phase considered as pseudo-fluid phase (Spalding, 1981).

MATHEMATICAL MODEL

The schematic diagram of the flow configuration is shown in Fig.1. The central primary jet is loaded with particles and the annular jet provides swirling air stream. The 2-D gas-solid two phase flow model can be obtained on the basis of the standard k-ε model of gas phase. The conservation equations of this model in cylindrical coordinates can be written as following (Huang et al., 1991).

Gas phase:

$$\frac{\partial}{\partial x}(\rho u \phi) + \frac{1}{r}\frac{\partial}{\partial r}(r\rho v \phi) = \frac{\partial}{\partial x}\left(\Gamma_\phi \frac{\partial \phi}{\partial x}\right) + \frac{1}{r}\frac{\partial}{\partial r}\left(\Gamma_\phi \frac{\partial \phi}{\partial r}\right) + S_\phi + S_{\phi p} \quad (1)$$

Particle phase:

$$\frac{\partial}{\partial x}(n_p u_p \phi_p) + \frac{1}{r}\frac{\partial}{\partial r}(r n_p v_p \phi_p) = \frac{\partial}{\partial x}\left(\Gamma_{\phi p}\frac{\partial \phi_p}{\partial x}\right) + \frac{1}{r}\frac{\partial}{\partial r}\left(\Gamma_{\phi p} r \frac{\partial \phi_p}{\partial r}\right) + S_{p\phi} \quad (2)$$

* Project supported by Zhejiang Provincial Natural Science Foundation, China (No. 598017).
† Author for correspondence, Fax: +86 – 0571 – 87951358; E-mail: fanjr@mail.hz.zj.cn

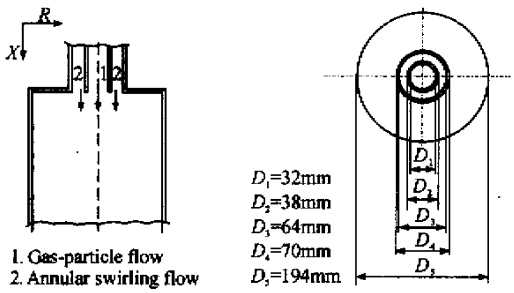

Fig.1 Flow configuration of swirling gas-solid two phase flow

The expressions of the different variables ϕ, ϕ_p of the equations above, their corresponding effective viscosity Γ_ϕ, $\Gamma_{\phi p}$ and source terms $(S_\phi + S_{\phi p})$, are given in Table 1, where $S_{p\phi}$ stands for the source term of the fluid phase acting on the particle phase.

Since the kinetic energy of the particle phase is mainly decided by the local kinetic energy of the gas phase, dimension analysis can be used to describe the particle phase turbulent viscosity γ_p as $\gamma_p = C_{\mu p} k_p^{\frac{1}{2}} k^{\frac{3}{2}}/\varepsilon$. The turbulent diffusion of the particle phase is expressed by the Fick Law, the product of the particle turbulent viscosity and the gradient of the particle mean density.

Table 1 Expressions of Φ, Γ, S in Eqs.(1) and (2)

$[\phi/\phi_p]$	$[\Gamma_\phi/\Gamma_{\phi p}]$	Source term $[S_\phi + S_{\phi p})/S_{p\phi}]$
1	0	–
u	μ_e	$-\frac{\partial p}{\partial x} + \frac{\partial}{\partial x}\left(\mu_e \frac{\partial u}{\partial x}\right) + \frac{1}{r}\frac{\partial}{\partial r}\left(r\mu_e \frac{\partial v}{\partial r}\right) + \rho_p(u_p - u)/\tau_{rp}$
v	μ_e	$-\frac{\partial p}{\partial r} + \frac{\partial}{\partial x}\left(\mu_e \frac{\partial u}{\partial r}\right) + \frac{1}{r}\frac{\partial}{\partial r}\left(r\mu_e \frac{\partial v}{\partial r}\right) - 2\mu_e \frac{v}{r^2} + \frac{\rho w^2}{r} + \rho_p(v_p - v)/\tau_{rp}$
w	μ_e	$-\frac{\rho v w}{r} - \frac{w}{r^2}\frac{\partial}{\partial r}(r\Gamma) - \rho_p(w_p - w)/\tau_{rp}$
k	μ_e/σ_k	$G_k - \rho\varepsilon + G_p$
ε	μ_e/σ_ε	$C_1\frac{\varepsilon}{k}(G_k + G_p) + C_2\rho\frac{\varepsilon^2}{k}$
n_p	γ_p/σ_p	0
u_p	$n_p\gamma_p$	$\frac{\partial}{\partial x}\left(n_p\gamma_p\frac{\partial u_p}{\partial x}\right) + \frac{1}{r}\frac{\partial}{\partial r}\left(rn_p\gamma_p\frac{\partial v_p}{\partial x}\right) + \frac{n_p}{\tau_{rp}}(u - u_p) + \frac{\partial}{\partial x}\left(u_p\frac{\gamma_p}{\sigma_p}\frac{\partial n_p}{\partial x}\right) + \frac{1}{r}\frac{\partial}{\partial r}\left(ru_p\frac{\gamma_p}{\sigma_p}\frac{\partial n_p}{\partial r}\right)$
v_p	$n_p\gamma_p$	$\frac{\partial}{\partial x}\left(n_p\gamma_p\frac{\partial u_p}{\partial r}\right) + \frac{1}{r}\frac{\partial}{\partial r}\left(rn_p\gamma_p\frac{\partial v_p}{\partial r}\right) + \frac{n_p}{\tau_{rp}}(v - v_p) + \frac{\partial}{\partial x}\left(v_p\frac{\gamma_p}{\sigma_p}\frac{\partial n_p}{\partial x}\right) + \frac{1}{r}\frac{\partial}{\partial r}\left(rv_p\frac{\gamma_p}{\sigma_p}\frac{\partial n_p}{\partial r}\right) + \frac{n_p w_p^2}{r} + n_p g$
w_p	$n_p\gamma_p$	$-\frac{n_p v_p w_p}{r} - \frac{w_p}{r^2}\frac{\partial}{\partial r}(rn_p\gamma_p) + \frac{n_p}{\tau_{rp}}(w - w_p)$
k_p	$n_p\gamma_p/\sigma_p$	$G_{kp} - n_p\varepsilon_p$

Where, $\mu_e = \mu + \mu_T$, $\mu_T = C_\mu \rho k^2/\varepsilon$; $\gamma_p = C_{\mu p} k_p^{\frac{1}{2}} k^{\frac{3}{2}}/\varepsilon$;

$$G_k = \mu_T\left\{2\left[\left(\frac{\partial u}{\partial x}\right)^2 + \left(\frac{\partial v}{\partial r}\right)^2 + \left(\frac{v}{r}\right)^2\right] + \left(\frac{\partial w}{\partial x} + \frac{r\partial}{\partial r}\left(\frac{w}{r}\right) + \left(\frac{\partial u}{\partial r} + \frac{\partial v}{\partial x}\right)^2\right\};$$

$$G_{kp} = n_p\gamma_p\left\{2\left[\left(\frac{\partial u_p}{\partial x}\right)^2 + \left(\frac{\partial v_p}{\partial r}\right)^2 + \left(\frac{v_p}{r}\right)^2\right] + \left(\frac{\partial w_p}{\partial x} + \frac{r\partial}{\partial r}\left(\frac{w_p}{r}\right) + \left(\frac{\partial u_p}{\partial r} + \frac{\partial v_p}{\partial x}\right)^2\right\};$$

$$G_p = -\frac{n_p m_p}{\tau_{rp}}\left[2(k - C_p^k\sqrt{kk_p}) + \frac{\gamma_p}{n_p\sigma_p}\left(u_p\frac{\partial n_p}{\partial x} + v_p\frac{\partial n_p}{\partial r}\right)\right];$$

$$\varepsilon_p = -\frac{2}{\tau_{rp}}(C_p^k\sqrt{kk_p} - k_p) - \frac{k_p}{n_p}\left[\frac{\partial}{\partial x}\left(\frac{\gamma_p}{\sigma_p}\frac{\partial n_p}{\partial x}\right) + \frac{1}{r}\frac{\partial}{\partial r}\left(r\frac{\gamma_p}{\sigma}\frac{\partial n_p}{\partial r}\right)\right];$$

$$\tau_{rp} = \tau'_{rp}(1 + Re_p^{\frac{2}{3}}/6)^{-1},\ Re_p = |\boldsymbol{u}_p - \boldsymbol{u}|\frac{\rho d_p}{\mu},\ \tau'_{rp} = \frac{d_p^2\rho_p}{18\mu};$$

Where u_p, u = particle and gas axial mean velocity; v_p, v = particle and gas radial mean velocity; w_p, w = particle and gas tangential mean velocity; k_p, k = particle and gas turbulent energy; γ_p, μ_e = particle and gas turbulent viscosity; τ_{rp} = particle stokesian response time; x, r = coordinates; n_p = particle mean number density; subscript p = particle.

$C_\mu = 0.09$, $C_1 = 1.44$, $C_2 = 1.92$, $\sigma_k = 1$, $\sigma_\varepsilon = 1.33$, $\sigma_p = 0.7$, $C_p^k = 0.75$, $C_{\mu p} = 0.0064$, $\mu = 18.08 \times 10^{-6}$(Pa•s).

Since the density ratio $\rho_p/\rho > 1000$, the Basset force, the added force, can be neglected. And the collisions between the particles can be ignored because of low particle loading. Since the gradient of the velocity is not very big, the Magnus force is neglected. It was concluded that the Saffman force should be considered only when the particle rotation is very high (Elghobashi et al., 1992, Shi, et al., 1989), so it was neglected too.

As conclued above, the reactions between the two phases considered in the equations are the drag force and the gravity. The drag force between the two phases and the gravity are added to the source term of the both phases' momentum equations (Mclaughlin, 1994, Stock, 1995). The drag force can be expressed as $F_D = \rho(u_p - u)/\tau_{rp}$.

The flow parameters of different cases are shown in Table 2. The boundary conditions are specified as follows. The inlet conditions are specified according to the experimental conditions (Sommerfeld et al., 1993). Symmetrical condition at the axis, fully developed conditions at the outlet and no slip conditions at the wall are taken for both phases. And the wall function approximations are adopted for near-wall grid nodes.

Table 2 Flow parameters of both phases

Phase	Flow condition	Flow parameter		
		Case 1	Case 2	Case 3
Air flow	Mass flow rate of the primary jet (g/s)		6.0	
	Mass flow rate of the secondary flow (g/s)		44.6	
	Swirl number		0.49	
Particle phase	Particle loading in the primary jet		0.17	
	Particle mean diameter (μm)	30	45	60
	Particle material density (kg/m^3)		2500	

RESULTS AND DISCUSSIONS

The computational results were obtained on a $x \times r = 50 \times 50$ mesh grid. The span of the computational domain in the streamwise direction was 1.0 m so that the outflow conditions could be taken as fully developed.

The results were compared with published experimental data (Sommerfeld et. al, 1993). Figs. 2 to 5 show the measured and calculated profiles of the gas phase when the particle mean diameter was 30μm. The agreement for velocity in the three directions was very good, except for the axial velocity fluctuation between x = 52 mm and x = 85 mm. The agreement for velocity fluctuation was reasonably good. The disagreement between the measurements and calculations could be due to the fact that the turbulence anisotropic characteristic becomes most intensive at those cross sections. And the standard k-ε model based on the isotropic hypothesis could not predict it exactly. Simulations using models based on anisotropic hypothesis or using LES (large eddy simulation) and DNS (direct numerical simulation) may yield more precise result.

Figs. 6 to 9 show the measurements and calculations when the particle mean diameter was 30μm. The agreement was fairly good too. The lines of the experimental data collapsed in the axial region at the last cross section. It was because there were too few particles to be detected by LDV (laser Doppler velocimeter). A gas bubble was observed in the experiment in this region. For the same reason as that for the gas phase, the predictions of the axial velocity fluctuation at the core re-

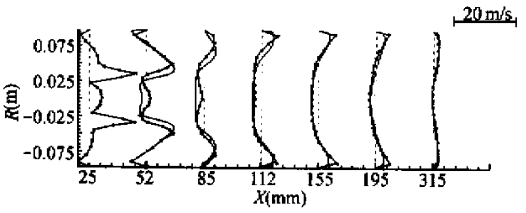

Fig.2 Measured and calculated axial gas velocity

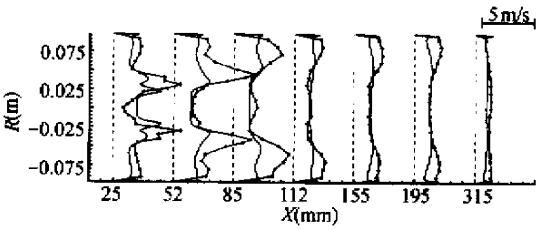

Fig.3 Measured and calculated axial gas velocity fluctuation

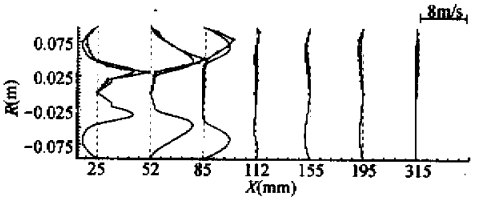

Fig.4 Measured and calculated radial gas velocity

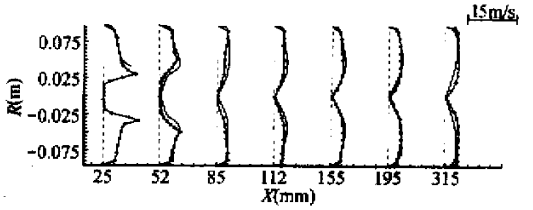

Fig.5 Measured and calculated tangential gas velocity

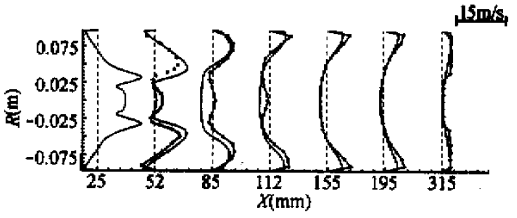

Fig.6 Measured and calculated axial particle velocity(30μm)

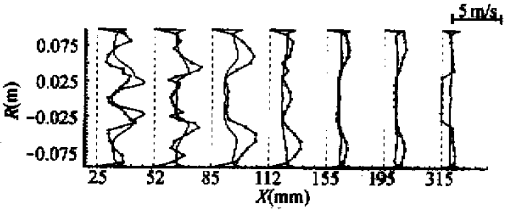

Fig.7 Measured and calculated axial particle velocity fluctuation (30μm)

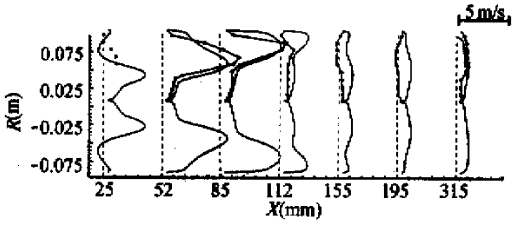

Fig.8 Measured and calculated radial particle velocity (30μm)

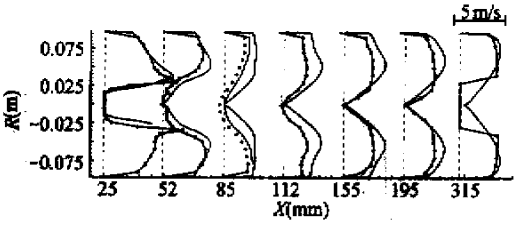

Fig.9 Measured and calculated tangential particle velocity (30μm)

gion near the cross section $x = 85$ mm were a little lower than the experiments. In some areas, the radial velocity in the experiments was negative but positive in the predictions. It can be explained that the particles near the wall region show particle characteristics more intensively when colliding with the wall. After collision with the wall the particles' radial velocity became negative. The collision was not very strong (which could be concluded from the low negative radial velocity), and would not affect the result very much.

The effect of the collision with the wall could also be seen when the mean diameter was 45μm (Fig. 10) and 60 μm (Fig. 11). The bigger the mean diameter, the stronger the collisions of the particles with the wall were. As a result, the difference between

measured and calculated radial velocity in those regions was more obvious.

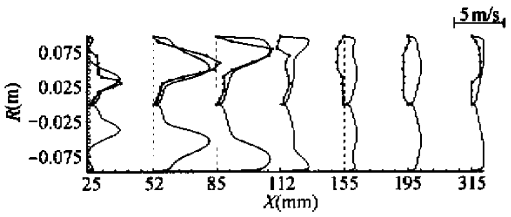

Fig.10 Measured and calculated radial particle velocity (45μm)

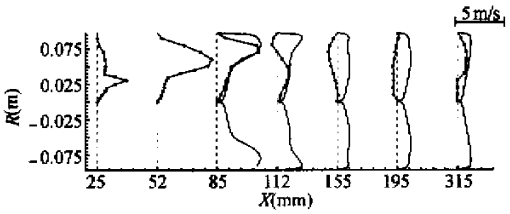

Fig.11 Measured and calculated radial particle velocity (60μm)

As shown in Figs.10 and 11 when particle mean diameters were 45 μm and 60 μm, although the particles' collisions with the wall were not considered, the calculated results still agree well with the experimental results. It shows that the pseudo-fluid characteristic of the particle phase is the leading characteristic in the particles' movement. If the mean diameter of the particles is not very big and the collisions of the particles with the wall are not very strong, the multi-fluid model can work fairly well.

CONCLUSIONS

A multi-fluid model was derived based on the standard simple phase model. The behavior of both phases in a confined swirling two-phase jet was simulated detailedly. The following conclusions:

1. The numerical simulations for different particle diameter showed good agreement with the experimental results for both phases. It shows the k-ε-k_p model can be applied to predict moderate swirling multi-phase flow.

2. The differences between calculation and experimental show there are some limits to using the model due to the isotropic hypothesis. Further studies should concentrate on establishing a model in which the anisotropic characteristic of turbulence is considered. LES or DNS can be the appropriate way to solve this problem.

3. The differences between measurements and calculations of the particle radial velocity show the particle phase has its own particle characteristic besides pseudo-fluid characteristic. The pseudo-fluid model of the particle phase can also be improved by considering the particle characteristics during collision with a wall.

References

Crowe, C.T., Troutt, T.R., Chung, J.N., 1996. Numerical models for two-phase flow. *Annu. Rev. Fluid. Mech.*, **28**: 149 – 158.

Elghobashi S.E., Truesdell G.C., 1992. Direct simulation of particle dispersion in decaying isotropic turbulence. *J. Fluid Mech.* **242**: 655 – 700.

He, H., Fan J.R., Cen, K.F., 2000. A numerical method for orthogonal grid generation by Laplace system. *Journal of Zhejiang University SCIENCE*. **1**(2): 125 – 128.

Huang, X.Q., 1989. Study of turbulent gas-particle jets and 3-D turbulent recirculating gas-particle flows. Doctor Dissertation of Tsinghua University.

Huang, X.Q., Zhou, L.X., 1991. Simulation of three-dimensional turbulent recirculating gas-particle flows by an energy equation model of particle turbulence. *Gas-Solid Flows* **121**: 261 – 265.

Jin, H.H., 1999. Research of charged gas-liquid two-phase turbulence jet and its application in pest controlling. Master discourse of Jiangsu University of Science and Technology.

Mclaughlin, F.B., 1994. Numerical computation of particle-turbulence interaction. *Int. J. Multiphase Flow* **20**(Suppl): 211 – 232.

Shi, X.G., Xu, X.C., Feng, J.K., 1989. Analysis of forces on particles moving in turbulent flow. *J. Engineering Thermalphysics* **10**(3): 320 – 325.

Sommerfeld, M., Qiu, H.H., 1993. Characterization of particle-laden, confined swirling flows by phase-doppler anemomentry and numerical calculation. *Int. J. Multiphase Flow* **19**: 1093 – 1127.

Spalding, D.B., 1981. A general purpose computer rogram for multidimensional one- and two-phase flows. *J. Math Comput. Simul.* **23**: 267 – 276.

Stock D.E., 1995. Freeman scholar lecture: Particle dispersion in gases. *J. Fluids Engr.* **117**: 657 – 666.

Zha, X.D., Fan, J.R., Sun, P., 2000. Numerical simulation on dense gas-particle riser flow. *Journal of Zhejiang University SCIENCE* **1**(1): 29 – 38.

Note: Explanation an apology to our readers: we'll use this article to replace that of 2002, first issue p.82 – 85, JZU(S).